

A new source of methylglyoxal in the aqueous phase

Maria Rodigast, Anke Mutzel, Janine Schindelka and Hartmut Herrmann*

*Leibniz Institute for Tropospheric Research (TROPOS), Atmospheric Chemistry Dept. (ACD), Permoserstr. 15,
D-04318 Leipzig, Germany*

*Corresponding author. Tel: +49-341-2717-7024; fax: +49-341-271799-7024.

E-mail address: herrmann@tropos.de

For submission to: Atmospheric Chemistry and Physics

First submitted on 27.10.2015

1 **Abstract**

2 Carbonyl compounds are ubiquitous in atmospheric multiphase system participating in gas, particle, and aqueous-
3 phase chemistry. One important compound is methyl ethyl ketone (MEK), as it is detected in significant amounts
4 in the gas phase as well as in cloud water, ice, and rain. Consequently, it can be expected that MEK influences the
5 liquid phase chemistry. Therefore, the oxidation of MEK and the formation of corresponding oxidation products
6 were investigated in the aqueous phase. Several oxidation products were identified from the oxidation with OH
7 radicals, including 2,3-butanedione, hydroxyacetone, and methylglyoxal. The molar yields were 29.5% for
8 2,3-butanedione, 3.0% for hydroxyacetone, and 9.5% for methylglyoxal. Since methylglyoxal is often related to
9 the formation of organics in the aqueous phase, MEK should be considered for the formation of aqueous secondary
10 organic aerosol (aqSOA). Based on the experimentally obtained data, a reaction mechanism for the formation of
11 methylglyoxal has been developed and evaluated with a model study. Besides known rate constants, the model
12 contains measured photolysis rate constants for MEK ($k_p = 5 \times 10^{-5} \text{ s}^{-1}$), 2,3-butanedione ($k_p = 9 \times 10^{-6} \text{ s}^{-1}$),
13 methylglyoxal ($k_p = 3 \times 10^{-5} \text{ s}^{-1}$), and hydroxyacetone ($k_p = 2 \times 10^{-5} \text{ s}^{-1}$). From the model predictions, a branching
14 ratio of 60/40 for primary/secondary H-atom abstraction at the MEK skeleton was found. This branching ratio
15 reproduces the experiment results very well, especially the methylglyoxal formation, which showed excellent
16 agreement. Overall, this study demonstrates MEK as a methylglyoxal precursor compound for the first time.
17

18 1. Introduction

19 In the last decades, carbonyl compounds have been a subject of intense research due to their ubiquitous abundance
20 and their effect on atmospheric chemistry and human health. They are emitted directly from biogenic and
21 anthropogenic sources or formed through the oxidation of hydrocarbons (e.g., Atkinson, 1997; Matthews and
22 Howell, 1981; Lipari et al., 1984; Ciccioli et al., 1993; Mopper and Stahovec, 1986; Carlier et al., 1986; Hallquist
23 et al., 2009). One carbonyl compound that is emitted from numerous and mainly biological sources is methyl ethyl
24 ketone (MEK). It is released from grass, clover (Kirstine et al., 1998; de Gouw et al., 1999), different types of
25 forests, and biomass burning processes (Khalil and Rasmussen, 1992; Warneke et al., 1999; Isidorov et al., 1985).
26 Anthropogenic emissions are also important MEK sources, such as artificial biomass burning (Andreae and
27 Merlet, 2001; Akagi et al., 2011; Yokelson et al., 2013; Brilli et al., 2014) and tobacco smoke (Buyske et al.,
28 1956; Yokelson et al., 2013). In addition, MEK is emitted into the atmosphere through the application as solvent
29 for the production of glue, resins, cellulose, rubber, paraffin wax and lacquer (Ware, 1988).

30 Tropospheric MEK gas-phase concentration was found to be in the range of 0.02 – 15 ppbv, depending
31 on the region (Grosjean et al., 2002; Riemer et al., 1998; Singh et al., 2004; Snider and Dawson, 1985; Goldan et
32 al., 1995; Grosjean et al., 1983; Grosjean, 1982; Müller et al., 2005; Feng et al., 2004). Singh et al. (2004)
33 measured a concentration in a remote region of 0.02 ppbv, whereas Grosjean et al. (1983) observed a MEK
34 concentration of 11.3 ppbv in Los Angeles. Brown et al. (1994) concluded that MEK is one of the major volatile
35 organic compounds (VOCs) in indoor air.

36 In addition to the gas-phase measurements, the concentrations measured in bulk water samples collected
37 at an open station near the Bahamas reached a concentration of $< 0.5 \text{ nmol L}^{-1}$ (Zhou and Mopper, 1997).
38 Furthermore, an enrichment of MEK in the surface micro layer was found with concentrations up to 2.28 nmol L^{-1}
39 (Zhou and Mopper, 1997). MEK was also investigated in ice, fog, and rain samples (Grosjean and Wright, 1983).
40 It was not found in fog but there were traces in rain water. In cloud water, a concentration of up to 650 nmol L^{-1}
41 was measured. This is supported by van Pinxteren et al. (2005), who measured a concentration of
42 70 to 300 nmol L^{-1} in cloud water. These studies concluded that the liquid-phase fraction of MEK is higher than
43 the expected fraction calculated according to the Henry constant.

44 The Henry constants at a temperature of $25 \text{ }^{\circ}\text{C}$ were found to vary between 7.7 and 21 M atm^{-1} in
45 numerous studies (Buttery et al., 1969; Snider and Dawson, 1985; Ashworth et al., 1988; Zhou and Mopper, 1990;
46 Morillon et al., 1999; Karl et al., 2002). However, Schütze and Herrmann (2004) estimated the Henry constant to
47 be between 23 and 50 M atm^{-1} , which is higher than the previous measured values found in the literature. This
48 higher Henry constant supports the conclusion from van Pinxteren et al. (2005) and tends to support the
49 investigation of MEK in the liquid phase as aqSOA precursor compound. AqSOA is formed through the oxidation
50 of organic compounds in the aqueous particle phase and is often related to missing SOA sources. These missing
51 sources are most likely responsible for the huge discrepancies between measured and calculated SOA burden. As
52 model results usually underestimate the SOA burden (Kanakidou et al., 2005; Goldstein and Galbally, 2007),
53 missing SOA sources have to be considered in such models to close this gap (Ervens et al., 2011; Herrmann et al.,
54 1999; Herrmann et al., 2015).

55 In the present study, the reaction of MEK with OH radicals in water was investigated. Based on the
56 experimentally obtained data, a reaction mechanism was developed to explain methylglyoxal formation. The

57 mechanism was included in a COPASI (Complex Pathway Simulator) model and evaluated by comparing the
58 experimentally obtained data and the model results.

59 2. Experimental

60 2.1 Chemicals and standards

61 Cyclohexanone-2,2,6,6-d₄ (98%), hydrochloric acid, and catalase from bovine liver (40000-60000 units mg⁻¹
62 protein) were obtained from Sigma-Aldrich (Hamburg, Germany). *O*-(2,3,4,5,6-
63 pentafluorobenzyl)hydroxylamine hydrochloride ($\geq 99\%$), 2,3-butanedione (99%), hydroxyacetone (90%), and
64 methylglyoxal (40% in water) were purchased from Fluka (Hamburg, Germany). Dichloromethane (Chromasolv
65 99.8%) and methyl ethyl ketone (99.7%) were obtained from Riedel-de Haen (Seelze, Germany), and hydrogen
66 peroxide (30% Suprapur[®]) was obtained from Merck KGaA (Darmstadt, Germany). Ultrapure water was used to
67 prepare the reaction solutions for the bulk reactor experiments and the stock solutions of the authentic standard
68 compounds (Milli-Q gradient A 10, 18.2 M Ω cm⁻¹, 3 ppb TOC, Millipore, USA).

69 2.2 Bulk reactor experiments

70 The aqueous-phase oxidation of MEK was conducted in a 300 mL batch reactor using the photolysis of hydrogen
71 peroxide (H₂O₂) as an OH radical source (Set 1). The experiments were conducted at a temperature of 298 K. For
72 the experiments, 0.1 mmol L⁻¹ of the precursor compound was mixed with 2 mmol L⁻¹ of H₂O₂. The solution was
73 then irradiated at $\lambda = 254$ nm for 4 hours to continuously generate OH radicals (500 W xenon-mercury lamp,
74 Andover Corporation Optical bandpass filter: L.O.T.- Oriel GmbH & Co. KG, Darmstadt, Germany). To obtain
75 time-resolved data, samples were taken once per hour (0 – 4 hours; number of repetitions $n = 3$) or in steps of
76 15 minutes ($n = 1$) and analyzed after derivatization using GC/MS. To avoid further reactions of the organics
77 present in the sample with remaining H₂O₂, 100 μ L of catalase (4 mg mL⁻¹ in water) were added to each sample.
78 Furthermore, a set of blank experiments was conducted to exclude that (a) MEK reacts with H₂O₂ (Set 2),
79 (b) identified oxidation products originate from photolysis (Set 3), (c) the photolysis of contaminants in the H₂O₂
80 solution results in the formation of organics (Set 4), and (d) oxidation of 2,3-butanedione or hydroxyacetone also
81 forms methylglyoxal (Set 5/6). To determine the photolysis rate constants of 2,3-butanedione, methylglyoxal, and
82 hydroxyacetone, the photolysis of these products was investigated as well with the setup used (Set 7). A complete
83 overview of the experiments conducted is given in Table 1.

84 2.3 Sample preparation

85 Two types of samples were taken over a period of 4 hours. For the first type of samples, 60 μ L of the reaction
86 mixture were diluted with 2940 μ L of water to avoid saturation of the GC/MS detector during the quantification
87 of MEK, 2,3-butanedione or hydroxyacetone. For the second type of samples, 3 mL of the reaction mixture were
88 taken and injected without any dilution to enable the identification and quantification of the formed carbonyl
89 compounds.

90 Samples of all sets were derivatized with 300 μ L of *o*-(2,3,4,5,6-pentafluorobenzyl)hydroxylamine
91 hydrochloride (PFBHA, 5 mg mL⁻¹) at room temperature (Rodigast et al., 2015). Cyclohexanone-2,2,6,6-d₄ was
92 used as an internal standard (150 μ L, 100 μ mol L⁻¹), and after 24 hours, a pH value of 1 was adjusted by adding
93 hydrochloric acid (37%) to the reaction mixture. The target compounds were extracted for 30 minutes with 250 μ L
94 of dichloromethane using an orbital shaker (1500 rpm, revolutions per minutes). Finally, 1 μ L of the organic phase

95 was used for GC/MS analysis. A 5-point calibration was performed for each chromatographic run using a series
96 of the standard solutions (MEK, methylglyoxal, 2,3-butanedione, and hydroxyacetone) with concentrations
97 ranging from 1 to 50 $\mu\text{mol L}^{-1}$.

98 2.4 Instrumentation

99 Derivatized carbonyl compounds were analyzed using a GC System (6890 Series Agilent Technologies, Frankfurt,
100 Germany) coupled with an electron ionization quadrupole mass spectrometer in splitless mode at a temperature
101 of 250 °C (Agilent 5973 Network mass selective detector, Frankfurt, Germany). They were separated with an HP-
102 5MS UI column (Agilent J & W GC columns, 30 m \times 0.25 mm \times 0.25 μm) using the following temperature
103 program: 50 °C isothermal for 2 minutes and elevated to 230 °C with 10 °C minute^{-1} . The temperature of 230 °C
104 was held for 1 minute, and the temperature gradient ended with 320 °C, which was held constant for 10 minutes.

105 2.4 Instrumentation

106 Derivatized carbonyl compounds were analysed using a GC System (6890 Series Agilent Technologies, Frankfurt,
107 Germany) coupled with an electron ionization quadrupole mass spectrometer (Agilent 5973 Network mass
108 selective detector, Frankfurt, Germany) in the splitless mode at a temperature of 250 °C. They were separated
109 with a HP-5MS UI column (Agilent J & W GC columns, 30 m \times 0.25 mm \times 0.25 μm) using the following
110 temperature program: 50 °C isothermal for 2 minutes and elevated to 230 °C with 10 °C minute^{-1} . The temperature
111 of 230 °C was held for 1 minute and the temperature gradient ended with 320 °C which was held constant for
112 10 minutes.

113 3. Results

114 3.1 Experimental results from bulk reactor

115 MEK was oxidized with OH radicals, and the decay of MEK was monitored by GC/MS. Fig. 1A shows the
116 consumption of the precursor compound MEK. As can be seen, MEK was almost consumed after 180 minutes of
117 reaction time. From the analysis of the collected samples, 2,3-butanedione, hydroxyacetone, and methylglyoxal
118 were observed as the most dominating oxidation products. The formation of methylglyoxal from the oxidation of
119 MEK was unexpected as it has not been reported in the literature before. Due to the relevance of methylglyoxal
120 for aqSOA formation, its formation was comprehensively characterized in the present study.

121 Nevertheless, in Fig. 1B, 2,3-butanedione was found as the main oxidation product of MEK reaching a
122 maximum yield of $\approx 29.5 \pm 6.0\%$ after 60 minutes. The small variations of the molar yields over the course of the
123 experiment might result from slight temperature changes during the experiment despite the reactor temperature
124 being controlled. However, the curve shape shows that the concentration of 2,3-butanedione starts to decrease
125 after 60 minutes, indicating further reactions of 2,3-butanedione. This decrease results in a molar yield of
126 $18.9 \pm 3.9\%$ at the end of the experiment (240 minutes).

127 A similar trend was observed for hydroxyacetone and methylglyoxal, as the concentration of
128 methylglyoxal was the highest after 15 minutes ($\approx 9.5\%$) and started to decrease afterwards. In comparison,
129 hydroxyacetone reached the highest concentration after 60 minutes with a molar yield of $3.0 \pm 2.6\%$. The standard
130 deviation of the determined molar yields of hydroxyacetone was high, and therefore, only after reaction times of
131 60 and 120 minutes could a molar yield of hydroxyacetone be determined.

132 Methylglyoxal and hydroxyacetone were completely consumed at the end of the experiment. The strong
133 decrease of the concentrations of the detected carbonyl compounds might result from the reaction with OH radicals
134 and/or from photolysis. Both mechanisms are most likely, as it has been demonstrated that the detected carbonyl
135 compounds react quickly with OH radicals (Lilie et al., 1968; Gligorovski and Herrmann, 2004; Doussin and
136 Monod, 2013; Monod et al., 2005; Ervens et al., 2003; Herrmann et al., 2005; Tan et al., 2010; Stefan and Bolton,
137 1999) and they are prone to photolysis (Faust et al., 1997; Tan et al., 2010). The photolysis rate constants of the
138 detected carbonyl compounds were determined in the present study because of the dependency on the setup used
139 (Set 7; see supplement S2 for more details). Methylglyoxal and hydroxyacetone showed higher photolysis rate
140 constants of $k_p = 3 \times 10^{-5} \text{ s}^{-1}$ and $k_p = 2 \times 10^{-5} \text{ s}^{-1}$ in comparison to 2,3-butanedione ($k_p = 9 \times 10^{-6} \text{ s}^{-1}$). This
141 indicates a faster decomposition compared to 2,3-butanedione of methylglyoxal and hydroxyacetone, which
142 showed a complete consumption at the end of the experiment (Fig. 1). 2,3-Butanedione was not completely
143 consumed during the reaction time of 4 hours, which might be a result of the lower photolysis rate constants.
144 Furthermore, during the photolysis of 2,3-butanedione and hydroxyacetone, methylglyoxal was found with molar
145 yields of $\approx 17\%$ and $\approx 19\%$, respectively (see Fig. S2, supplement S2). Due to the low molar yield of
146 hydroxyacetone during the oxidation of MEK ($\approx 3\%$) and the slow photolysis rate constant of 2,3-butanedione,
147 these processes are of minor importance for the methylglyoxal yield.

148 For 2,3-butanedione, a huge discrepancy of the rate constants for the OH radical oxidation can be found
149 between the different literature studies. They vary by one order of magnitude in a range of $k = 1.4 \times 10^8 \text{ M}^{-1} \text{ s}^{-1}$
150 (Gligorovski and Herrmann, 2004) up to $k = 1.86 \times 10^9 \text{ M}^{-1} \text{ s}^{-1}$ (Doussin and Monod, 2013). Rate constants were
151 determined between $k = 5.3 \times 10^8 \text{ M}^{-1} \text{ s}^{-1}$ and $k = 1.1 \times 10^9 \text{ M}^{-1} \text{ s}^{-1}$ for methylglyoxal (Monod et al., 2005; Ervens
152 et al., 2003; Herrmann et al., 2005; Tan et al., 2010) and between $k = 0.8 \times 10^9 \text{ M}^{-1} \text{ s}^{-1}$ and $k = 1.2 \times 10^9 \text{ M}^{-1} \text{ s}^{-1}$
153 for hydroxyacetone (Stefan and Bolton, 1999; Herrmann et al., 2005). In consideration of the similar rate constant
154 for 2,3-butanedione determined by Lilie et al. (1968) ($k = 1.8 \times 10^8 \text{ M}^{-1} \text{ s}^{-1}$) and Gligorovski and Herrmann (2004)
155 ($k = 1.4 \times 10^8 \text{ M}^{-1} \text{ s}^{-1}$), 2,3-butanedione revealed a slower OH radical reaction than methylglyoxal and
156 hydroxyacetone. This is in good agreement with the experimental results obtained in the present study.

157 Since 2,3-butanedione is the main oxidation product, it was necessary to investigate the contribution of
158 2,3-butanedione to the product distribution, especially for the formation of methylglyoxal. In the oxidation of 2,3-
159 butanedione (Set 5), no methylglyoxal was detected in the GC/MS chromatogram over a reaction period of
160 240 min (Fig. 2). Consequently, a contribution of 2,3-butanedione to the methylglyoxal formation could be
161 excluded.

162 Despite the low molar yield of hydroxyacetone during MEK oxidation, the oxidation of hydroxyacetone
163 was investigated for methylglyoxal formation as well (Herrmann et al., 2005; Schaefer et al., 2012; Set 6). During
164 the oxidation, a molar yield of 100% was found after a reaction time of 60 minutes (see supplement S3, Fig. S3).
165 After 60 minutes of reaction time, the molar yield of methylglyoxal decreases through further reactions, as was
166 observed during MEK oxidation. However, due to the low molar yield of hydroxyacetone (3.0%), the oxidation
167 has only minor importance for the observed molar yield of methylglyoxal.

168 To ensure methylglyoxal was only formed during the oxidation of MEK, an experiment was conducted
169 to investigate the non-radical reaction of MEK with H_2O_2 in the dark (Set 2). During this experiment, no
170 decomposition of MEK was observed, excluding the non-radical reaction of MEK with H_2O_2 as a source of
171 methylglyoxal. Furthermore, the photolysis of MEK has to be considered as a source for methylglyoxal. Hence,

172 the photolysis of MEK was studied at $\lambda = 254$ nm (Set 3). As can be seen in Fig. 3, the photolysis of MEK leads
173 to the formation of 2,3-butanedione with a molar yield of $\approx 2.2\%$ indicating that the photolysis of MEK is an
174 additional source. No further carbonyl compounds were detected from the photolysis of MEK, and thus, the
175 photolysis of MEK can be excluded as a methylglyoxal source. The blank experiment (Set 4) indicated the absence
176 of methylglyoxal as well.

177 In summary, the oxidation of MEK constitutes a source for methylglyoxal, and due to the high
178 concentration of MEK in cloud water ($70 - 650$ nmol L⁻¹; Grosjean and Wright, 1983; van Pinxteren et al., 2005),
179 this source is of atmospheric relevance. Due to the molar yields of 9.5% for methylglyoxal, 29.5% for 2,3-
180 butanedione, and 3.0% for hydroxyacetone, $\approx 42\%$ of the oxidation products of MEK could be elucidated in the
181 present study with only these carbonyl compounds (Table 2). This highlights the importance of carbonyl
182 compounds for the aqueous phase chemistry. Based on the experimental findings, a reaction mechanism was
183 developed to describe the formation of methylglyoxal (Fig. 4).

184 3.2 Oxidation mechanism and model description

185 According to the structure of MEK, the OH radical attack can proceed at three different positions (Fig. 4; H-atoms
186 at carbons 1, 3, and 4). For the present study, only the attack at carbons 3 and 4 is considered because these
187 processes lead to the formation of the observed products (Fig. 4). Note that the abstraction of a hydrogen atom at
188 carbon 3 leads to a secondary alkyl radical (A), whereas at the terminal carbon, a primary alkyl radical is formed
189 (B). The branching ratios for the formation of the primary and secondary alkyl radicals will be discussed in detail
190 in the next section (Sect. 3.2.1).

191 The primary and secondary alkyl radicals react rapidly with oxygen to form alkylperoxy radicals. The alkylperoxy
192 radical recombines to a tetroxide and reacts further in three different ways, including the formation of an carbonyl
193 compound and an alcohol (i), the formation of two carbonyl compounds and H₂O₂ (ii), and the decomposition into
194 an alkoxy radical (iii) (von Sonntag and Schuchmann, 1991). The decomposition of the tetroxide into a peroxide
195 and oxygen was not considered further due to the minor importance of this process (von Sonntag and Schuchmann,
196 1997). The secondary and primary alkylperoxy radicals can react with HO₂, forming organic hydroperoxides. The
197 organic peroxides react with OH radicals or photolyze, resulting in the formation of an alkoxy radical or tetroxide
198 that can react further, as described before through pathways i–iii. The described mechanism was included in a
199 COPASI model to examine the developed oxidation mechanism, the decomposition of the precursor compound,
200 and the formation of the observed products. Table 3 shows the considered reactions, the rate constants, and their
201 references. Only the reactions leading to the formation of the products identified are discussed in detail.
202 Surprisingly, the products 3-oxobutanal and hydroxybutanone were not observed during the experiments. Since
203 3-oxobutanal contains two carbonyl groups, two derivatives can be formed, including one (mass to charge ratio
204 m/z 281; M⁺) or two (m/z 476; M⁺) derivatized groups. Hydroxybutanone has one carbonyl group with a
205 derivatized m/z 283 (M⁺). As can be seen in Fig. 5, m/z 283 was not found in the extracted ion chromatogram
206 (EIC). Furthermore, m/z 281 and 476 can be detected in the EIC of the bulk reactor samples, but they can also be
207 found in the EIC of the authentic standard compounds. The sample of the authentic standard compounds does not
208 contain hydroxybutanone and 3-oxobutanal. According to the comparison of the EIC of the bulk reactor samples
209 and the authentic standard, it can be assumed that m/z 281 and 476 are fragments of the internal standard and 2,3-
210 butandione. No additional signals in the EIC of the samples were detected at m/z 281, 283, and 476, and thus, 3-

211 oxobutanal and hydroxybutanone are not formed during the experiment. Hence, their formation pathways were
212 excluded from the model.

213 3.2.1 HO_x chemistry and OH radical attack

214 The relevant reactions for HO_x chemistry according to R1-R6 are included in the mechanism. OH radicals were
215 formed through the photolysis of H₂O₂ at $\lambda = 254$ nm with measured photolysis rate constants of $k_p = 7.6 \times 10^{-6} \text{ s}^{-1}$
216 (R1, see supplement S1). The formed OH radicals react further with MEK in a first oxidation step, leading to the
217 formation of a primary (R7) and secondary alkyl radical (R8). The rate constants were postulated by
218 Herrmann et al. (2005) to be $k = 1.17 \times 10^8 \text{ M}^{-1} \text{ s}^{-1}$ and $k = 1.3 \times 10^9 \text{ M}^{-1} \text{ s}^{-1}$ for the formation of the primary and
219 secondary alkyl radicals, respectively. This is in good agreement with the model study by Sebbar et al., who
220 postulated that the H-atom abstraction most likely proceeds at the secondary carbon of MEK (Sebbar et al., 2014;
221 Sebbar et al., 2011) due to the lower C-H bond dissociation energy ($\approx 377 \text{ kJ mol}^{-1}$, C4) in comparison to the
222 primary carbon atom ($\approx 423 \text{ kJ mol}^{-1}$, C3). In the present study, a rate constant $k = 1.5 \times 10^9 \text{ M}^{-1} \text{ s}^{-1}$ (Gligorovski
223 and Herrmann, 2004) was used, and the branching ratio was varied from 60/40 to 10/90 for the primary/secondary
224 H-atom abstraction.

225 The results are shown in Fig. 6 and discussed based on the molar yields of the products. As can be seen
226 for 2,3-butanedione (Fig. 6A), a branching ratio of 60% for the primary H-atom abstraction and 40% for the
227 secondary H-atom abstraction leads to lower molar yields, whereas the molar yields start to increase with an
228 increasing fraction of secondary H-atom abstraction. According to the mechanism (Fig. 4), 2,3-butanedione is
229 only formed via secondary H-atom abstraction, and thus, it is feasible to reach higher molar yields with a higher
230 fraction of secondary H-atom abstraction. However, with an increasing secondary H-atom abstraction, the
231 experimentally determined concentration was increasingly overestimated, especially at the beginning of the
232 experiment. After 60 minutes of reaction time, the highest experimentally determined molar yield ($29.5 \pm 6.0\%$)
233 was overestimated by a factor of ≈ 2 with a ratio of 10/90 for primary/secondary H-atom abstraction (molar yield
234 $\approx 49.9\%$), whereas a ratio of 60/40 resulted in reasonably good agreement (molar yield $\approx 23.7\%$). Based on this,
235 a branching ratio of 60/40 for primary/secondary H-atom abstraction was used in the present model.

236 In contrast, methylglyoxal molar yields were increasingly underestimated with an increasing fraction of
237 secondary H-atom abstraction (Fig. 6B). Thus, after 15 minutes of reaction time, the experimental molar yield
238 ($\approx 9.5\%$) was underestimated by a factor of ≈ 5 with a higher fraction of the secondary H-atom abstraction (molar
239 yield $\approx 2\%$). In comparison with a ratio of 60/40 for primary/secondary H-atom abstraction, a molar yield of
240 $\approx 11.4\%$ was observed, which is in good agreement with the experiment. Overall, the branching ratio of 60/40
241 (primary/secondary H-atom abstraction) resulted in reasonable agreement for 2,3-butanedione and in an excellent
242 conformity to the methylglyoxal molar yields. This shows the importance of the primary H-atom abstraction as
243 the main decomposition pathway of MEK and thus for methylglyoxal formation.

244 The primary and secondary alkyl radicals react further with oxygen (R9/R21) with a rate constant of
245 $k = 3.1 \times 10^9 \text{ M}^{-1} \text{ s}^{-1}$ (Zegota et al., 1986; Glowa et al., 2000), which was reported for the formation of
246 acetylperoxy radicals. The rate constants of the acetylperoxy radical were used for the formation of the
247 primary alkylperoxy radical (R9) and further reactions of the alkylperoxy radical because of their structural
248 similarity. They were also applied by Glowa et al. (2000) for the formation of the secondary alkylperoxy radical
249 of MEK. Further reactions of the primary and secondary alkylperoxy radicals resulting in different oxidation
250 products will be discussed in detail in the following section (Sect. 3.2.2 and 3.2.3).

251 *3.2.2 Oxidation of MEK leading to the formation of methylglyoxal and hydroxyacetone*

252 Only the formation of the alkoxy radical (iii; R10) leads to the formation of methylglyoxal. The alkoxy radical
253 further reacts rapidly with oxygen into an acetylperoxy radical under elimination of formaldehyde. The
254 acetylperoxy radicals can recombine again to form a tetroxide (Schaefer et al., 2012). The latter is able to
255 decompose through pathways i–iii, which are illustrated in R11–R13. Consequently, the decomposition of the
256 tetroxide can explain the formation of hydroxyacetone and methylglyoxal (R11; $k = 2 \times 10^8 \text{ M}^{-1} \text{ s}^{-1}$; Zegota et al.,
257 1986), methylglyoxal (R12; $k = 4 \times 10^7 \text{ M}^{-1} \text{ s}^{-1}$; Zegota et al., 1986), and methylglyoxal and hydrogen peroxide
258 (R13; $k = 4 \times 10^8 \text{ M}^{-1} \text{ s}^{-1}$; Zegota et al., 1986; Schaefer et al., 2012).

259 In addition to the discussed pathway, the primary alkylperoxy radical has the opportunity to react with
260 HO_2 instead of the recombination, forming an organic hydroperoxide (R14). The rate constant was reported by
261 von Sonntag and Schuchmann (1991) to be from $10^7 \text{ M}^{-1} \text{ s}^{-1}$ up to $10^9 \text{ M}^{-1} \text{ s}^{-1}$. For the primary alkylperoxy radical,
262 $k = 1 \times 10^7 \text{ M}^{-1} \text{ s}^{-1}$ was used as it led to the best agreement of the experimental data and the model results. The
263 formed peroxide can react with OH radicals (R15) or photolyze (R16). The same rate constant
264 ($k = 2.7 \times 10^7 \text{ M}^{-1} \text{ s}^{-1}$) as that for the OH radical oxidation of H_2O_2 was used for R15 due to a lack of literature
265 data. According to the assumption by Monod et al. (2007), the rate constant for the photolysis of the formed
266 peroxide (R16) was defined to be 1/10 of the photolysis rate constants of hydrogen peroxide. Thus, a photolysis
267 rate constant of $k_p = 7.6 \times 10^{-7} \text{ s}^{-1}$ was included in the model. This was used as a first approximation due to a lack
268 of literature data for the formed hydroperoxides. The photolysis of the organic peroxide leads to the formation of
269 formaldehyde, OH radicals, and an acetyl radical, which reacts further with oxygen (R17) to form an
270 acetylperoxy radical ($k = 3.1 \times 10^9 \text{ M}^{-1} \text{ s}^{-1}$; Zegota et al., 1986; R19) and subsequently methylglyoxal
271 (R18 – 20).

272 *3.2.3 Oxidation of MEK leading to the formation of methylglyoxal and 2,3-butanedione*

273 As described for the primary alkylperoxy radical, the secondary alkylperoxy radical recombines and forms a
274 tetroxide. This reacts to form either (i) 2,3-butanedione and acetoin (R22) or (ii) 2,3-butanedione and hydrogen
275 peroxide (R23) and is considered with rate constants of $k = 2.5 \times 10^8 \text{ M}^{-1} \text{ s}^{-1}$ and $k = 4.5 \times 10^8 \text{ M}^{-1} \text{ s}^{-1}$ (Glowa et
276 al., 2000). The tetroxide can decompose into an alkoxy radical as well (iii) and react further to form 2,3-
277 butanedione, methylglyoxal, a methyl radical, and HO_2 (R24; $k = 5 \times 10^7 \text{ M}^{-1} \text{ s}^{-1}$; Glowa et al., 2000). The rate
278 constants postulated by Glowa et al. (2000) are derived from the branching ratios determined by Zegota et al.
279 (1986) for acetone. Glowa et al. (2000) simulated the concentration profiles of MEK and the corresponding
280 products and postulated the rate coefficient used in the present model study. The secondary alkylperoxy radical
281 also has the opportunity to react with HO_2 to form an organic peroxide (R25), which photolyzes (R26;
282 $k = 7.6 \times 10^{-7} \text{ s}^{-1}$) or reacts further with OH radicals (R28; $k = 2.7 \times 10^7 \text{ M}^{-1} \text{ s}^{-1}$). Through the photolysis, an
283 alkoxy radical was formed that leads to methylglyoxal, 2,3-butanedione, a methyl group, and HO_2 radicals
284 (R27; $k = 4 \times 10^7 \text{ M}^{-1} \text{ s}^{-1}$).

285 *3.2.4 Further reactions and photolysis of formed oxidation products and MEK*

286 The products 2,3-butanedione, methylglyoxal, and hydroxyacetone positively identified by GC/MS analysis might
287 also react further, forming a variety of oxidation products. The rate constant of methylglyoxal with OH radicals
288 is given in the range of $k = 5.3 \times 10^8 \text{ M}^{-1} \text{ s}^{-1}$ to $k = 1.1 \times 10^9 \text{ M}^{-1} \text{ s}^{-1}$ (Monod et al., 2005; Ervens et al., 2003;
289 Herrmann et al., 2005; Tan et al., 2010), whereas a rate constant of $k = 5.3 \times 10^8 \text{ M}^{-1} \text{ s}^{-1}$ (R29; Monod et al., 2005)

290 leads to the best agreement between the experimental data and the model results. In comparison, the rate constants
291 determined by Ervens et al. (2003), Herrmann et al. (2005), and Tan et al. (2010) resulted in an underestimation
292 of the molar yield. Methylglyoxal also has the opportunity to photolyze. The photolysis is included with
293 $k_p = 3 \times 10^{-5} \text{ s}^{-1}$ (R30) in the present model.

294 2,3-Butanedione is also prone to OH radical oxidation and photolysis. As discussed, a huge discrepancy
295 exists in the rate constants for the reaction of OH radicals with 2,3-butanedione (Lilie et al., 1968; Doussin and
296 Monod 2013; Gligorovski and Herrmann, 2004). In the present study, the value of $k = 1.4 \times 10^8 \text{ M}^{-1} \text{ s}^{-1}$ (R31)
297 determined by Gligorovski and Herrmann (2004) was used. The higher rate constants reported by Lilie et al.
298 (1968) and Doussin and Monod (2013) resulted in consumption that was too fast. The photolysis was included
299 with a rate constant of $k_p = 9 \times 10^{-6} \text{ s}^{-1}$ in the COPASI model (R32). It should be mentioned that methylglyoxal
300 was formed during the photolysis of 2,3-butanedione. However, the photolysis was too small to contribute
301 significantly to methylglyoxal formation. For more details, see supplement S2.

302 The oxidation of hydroxyacetone with OH radicals was also considered in the model study with a rate
303 constant of $k = 8 \times 10^8 \text{ M}^{-1} \text{ s}^{-1}$ (R33; Stefan and Bolton, 1999). During the experiment, methylglyoxal was formed
304 with 100% molar yield. Thus, the reaction of hydroxyacetone to methylglyoxal was included in the model study.
305 The photolysis of hydroxyacetone was measured with a rate of $k_p = 2 \times 10^{-5} \text{ s}^{-1}$, leading to methylglyoxal with a
306 molar yield of $\approx 19\%$ (R34). The photolysis rate constant of MEK was measured as $k_p = 5 \times 10^{-5} \text{ s}^{-1}$ (see
307 supplement S2, Fig. S1). During the experiment, 2,3-butanedione was found with a molar yield of 2.2%. Thus,
308 the reaction of MEK leading to 2,3-butanedione was included in the model study (R35).

309 3.3 Model results and comparison with the experimental dataset

310 The described reactions are included in a model, and the decomposition of MEK and molar yields of
311 formed products were compared to the experimentally obtained data (Fig. 7). The model was not validated with
312 the time course of hydroxyacetone due to the high standard deviation of the experimental results. The comparison
313 of the model study and the experiment showed very good agreement for the consumption of MEK (Fig. 7A).
314 There is also good agreement for the formation of methylglyoxal and limited agreement for the molar yields of
315 2,3-butanedione. The initial high molar yield of 2,3-butanedione is reflected well (Fig. 7B). Thus, after 60 minutes
316 of reaction time, molar yields of 23.7% in the model study and $29.5 \pm 6.0\%$ in the experiment were reached. Under
317 consideration of the standard deviation, this is in good agreement with the COPASI model.

318 The determined molar yields up to a reaction time of 120 minutes showed very good conformity with the
319 experiment (18.2% and $22.1 \pm 9.0\%$). The temporal behavior shows that the determined molar yield in the model
320 study is somewhat lower towards the end of the experiment. Hence, it is possible that there are other reaction
321 pathways that lead to higher molar yields of 2,3-butanedione at the end of the experiment, which are not
322 considered in the model study as of now. Good agreement between the model results and experiment was observed
323 for methylglyoxal (Fig. 7C). The curve shapes are very similar, and hence, fast formation and decomposition of
324 methylglyoxal were found in the model study and in the experiment. After 15 minutes of reaction time, a molar
325 yield of 9.5% was found in the experiment. In comparison, the model study resulted in a molar yield of 11.4%,
326 which is in good agreement with the experiment and validates the COPASI model.

327 **4. Atmospheric relevance**

328 The sources of methylglyoxal in the aqueous phase are thus-far not fully elucidated. Methylglyoxal can originate
329 in the atmospheric aqueous phase through i) uptake from the gas phase, and/or ii) formation in the aqueous phase.
330 The importance of the uptake from the gas into the aqueous phase is discussed in the literature but large
331 discrepancies can be found. Kroll et al. (2005) investigated the uptake of methylglyoxal on inorganic seed particles
332 under varying relative humidity. It was found that the uptake was not relevant for methylglyoxal even under high
333 relative humidity. Contrary, Zhao et al. (2006) measured an uptake coefficient of $\gamma = 7.6 \times 10^{-3}$ on acidic solution.
334 They found an irreversible uptake, which decreases with increasing acidity. Fu et al. (2008, 2009) determined an
335 uptake coefficient on aqueous particles and cloud droplets $\gamma = 2.9 \times 10^{-3}$, which is in good agreement with the
336 uptake coefficient measured by Zhao et al. (2006). Lin et al. (2014) modelled an uptake coefficient for several
337 case studies with different multiphase process mechanisms. The uptake coefficient in deliquescent particles was
338 determined to be $\gamma = 1.47 - 2.92 \times 10^{-5}$. Overall, γ was two orders of magnitude lower compared to the values
339 determined by Zhao et al. (2006) and Fu et al. (2008, 2009) showing the discrepancies between the different
340 studies available in literature.

341 The in-situ formation of methylglyoxal in the aqueous phase could be an important source as well (Blando and
342 Turpin, 2000; Sempere and Kawamura 1994). Within the present study, MEK was found as a new precursor
343 compound for methylglyoxal in the aqueous phase yielding methylglyoxal with a molar yield of 9.5%. Although
344 the Henry constant of MEK (up to $K_H = 50 \text{ M atm}^{-1}$, Schütze and Herrmann, 2004) is lower compared to
345 methylglyoxal ($K_H = 3.7 \times 10^3 \text{ M atm}^{-1}$, Betterton and Hoffmann, 1988), van Pinxteren et al. (2005) found higher
346 concentrations in cloud water as it was expected. Thus, the phase transfer of MEK from the gas in the aqueous
347 phase could be more important as currently derived from the available Henry constants. Besides the phase transfer,
348 the in-situ formation of MEK in aqueous phase formation might also represents an important source.

349 As, the oxidation of MEK yielding methylglyoxal has not been studied much before, it should be considered as a
350 formation process of methylglyoxal.

351

352 **5. Summary**

353 In the present study, MEK was identified as a new source for methylglyoxal in the aqueous phase. It was
354 demonstrated that methylglyoxal originates directly from MEK oxidation and not from side reactions such as
355 photolysis or non-radical reactions. A molar yield of $\approx 9.5\%$ was determined during the oxidation. Based on the
356 experimental results, a reaction mechanism could be developed. The calculations with a COPASI model supported
357 the experimental results and confirm MEK as a precursor compound for methylglyoxal in aqueous medium.

358 Further carbonyl compounds could be identified and quantified. 2,3-Butanedione was found as the main
359 oxidation product (molar yield $\approx 29.5\%$) and was formed during the photolysis of MEK as well. As a further
360 oxidation product, hydroxyacetone was identified and was formed with a molar yield of $\approx 3.0\%$ during the
361 oxidation of MEK.

362 The oxidation mechanism of MEK in aqueous solution was elucidated, and MEK was demonstrated to
363 be as a precursor compound for methylglyoxal in the aqueous phase. Regarding the important role of
364 methylglyoxal for the aqSOA formation, MEK has to be considered for aqSOA as well, which could be a next
365 step in reducing the underestimation of the SOA burden by model studies.

366 5. Acknowledgements

367 This study was supported by the Scholarship program of the German Federal Environmental Foundation
368 (Deutsche Bundesstiftung Umwelt, DBU; grant number 20013/244).

369 References

- 370 Akagi, S. K., Yokelson, R. J., Wiedinmyer, C., Alvarado, M. J., Reid, J. S., Karl, T., Crounse, J. D., and Wennberg,
371 P. O.: Emission factors for open and domestic biomass burning for use in atmospheric models, *Atmos. Chem.*
372 *Phys.*, 11, 4039-4072, 10.5194/acp-11-4039-2011, 2011.
- 373 Andreae, M. O., and Merlet, P.: Emission of trace gases and aerosols from biomass burning, *Glob. Biogeochem.*
374 *Cycle*, 15, 955-966, 10.1029/2000gb001382, 2001.
- 375 Ashworth, R. A., Howe, G. B., Mullins, M. E., and Rogers, T. N.: Air water partitioning coefficients of organics
376 in dilute aqueous-solutions, *J. Hazard. Mater.*, 18, 25-36, 10.1016/0304-3894(88)85057-x, 1988.
- 377 Atkinson, R.: Gas-phase tropospheric chemistry of volatile organic compounds .I. Alkanes and alkenes, *J. Phys.*
378 *Chem. Ref. Data*, 26, 215-290, 1997.
- 379 Blando, J. D., and Turpin B. J.: Secondary organic aerosol formation in cloud and fog droplets: a literature
380 evaluation of plausibility, *Atmos. Environ.*, 34, 1623-1632, 2000.
- 381 Brilli, F., Gioli, B., Ciccioli, P., Zona, D., Loreto, F., Janssens, I. A., and Ceulemans, R.: Proton Transfer Reaction
382 Time-of-Flight Mass Spectrometric (PTR-TOF-MS) determination of volatile organic compounds (VOCs)
383 emitted from a biomass fire developed under stable nocturnal conditions, *Atmospheric Environment*, 97, 54-
384 67, 10.1016/j.atmosenv.2014.08.007, 2014.
- 385 Brown, S. K., Sim, M. R., Abramson, M. J., and Gray, C. N.: Concentrations of volatile organic-compounds in
386 indoor air - a review, *Indoor Air-Int. J. Indoor Air Qual. Clim.*, 4, 123-134, 10.1111/j.1600-0668.1994.t01-2-
387 00007.x, 1994.
- 388 Buttery, R. G., Ling, L. C., and Guadagni, D. G.: Food volatiles - volatilities of aldehydes ketones and esters in
389 dilute water solution, *J. Agric. Food Chem.*, 17, 385-&, 10.1021/jf60162a025, 1969.
- 390 Buyske, D. A., Owen, L. H., Wilder, P., and Hobbs, M. E.: Chromatography of the 2,4-dinitrophenylhydrazones
391 of some aldehydes and ketones in tobacco smoke, *Anal. Chem.*, 28, 910-913, 10.1021/ac60113a040, 1956.
- 392 Carlier, P., Hannachi, H., and Mouvier, G.: The chemistry of carbonyl-compounds in the atmosphere - a review,
393 *Atmospheric Environment*, 20, 2079-2099, 10.1016/0004-6981(86)90304-5, 1986.
- 394 Christensen, H., Sehested, K., and Corfitzen, H.: Reactions of hydroxyl radicals with hydrogen-peroxide at
395 ambient and elevated-temperatures, *J. Phys. Chem.*, 86, 1588-1590, 10.1021/j100206a023, 1982.
- 396 Christensen, H., and Sehested, K.: HO₂ and O₂- radicals at elevated-temperatures, *J. Phys. Chem.*, 92, 3007-3011,
397 10.1021/j100321a060, 1988.
- 398 Ciccioli, P., Brancaleoni, E., Frattoni, M., Cecinato, A., and Brachetti, A.: Ubiquitous occurrence of semivolatile
399 carbonyl-compounds in tropospheric samples and their possible sources, *Atmospheric Environment Part a-*
400 *General Topics*, 27, 1891-1901, 10.1016/0960-1686(93)90294-9, 1993.
- 401 de Gouw, J. A., Howard, C. J., Custer, T. G., and Fall, R.: Emissions of volatile organic compounds from cut
402 grasses and clover are enhanced during the drying process, *Geophysical Research Letters*, 26, 811-814, 1999.
- 403 Doussin, J. F., and Monod, A.: Structure-activity relationship for the estimation of OH-oxidation rate constants
404 of carbonyl compounds in the aqueous phase, *Atmos. Chem. Phys.*, 13, 11625-11641, 10.5194/acp-13-11625-
405 2013, 2013.
- 406 Elliot, A. J., and Buxton, G. V.: Temperature-dependence of the reactions OH + O₂⁻ and OH + HO₂ in water up
407 to 200 °C, *J. Chem. Soc.-Faraday Trans.*, 88, 2465-2470, 10.1039/ft9928802465, 1992.
- 408 Ervens, B., Gligorovski, S., and Herrmann, H.: Temperature-dependent rate constants for hydroxyl radical
409 reactions with organic compounds in aqueous solutions, *Phys. Chem. Chem. Phys.*, 5, 1811-1824,
410 10.1039/b300072a, 2003.
- 411 Ervens, B., Turpin, B. J., and Weber, R. J.: Secondary organic aerosol formation in cloud droplets and aqueous
412 particles (aqSOA): a review of laboratory, field and model studies, *Atmos. Chem. Phys.*, 11, 11069-11102,
413 10.5194/acp-11-11069-2011, 2011.
- 414 Faust, B. C., Powell, K., Rao, C. J., and Anastasio, C.: Aqueous-phase photolysis of biacetyl (An α -dicarbonyl
415 compound): A sink for biacetyl, and a source of acetic acid, peroxyacetic acid, hydrogen peroxide, and the
416 highly oxidizing acetylperoxyl radical in aqueous aerosols, fogs, and clouds, *Atmospheric Environment*, 31,
417 497-510, 1997.
- 418 Feng, Y. L., Wen, S., Wang, X. M., Sheng, G. Y., He, Q. S., Tang, J. H., and Fu, J. M.: Indoor and outdoor
419 carbonyl compounds in the hotel ballrooms in Guangzhou, China, *Atmospheric Environment*, 38, 103-112,
420 10.1016/j.atmosenv.2003.09.061, 2004.

421 Fu, T-M., Jacob, D. J., Wittrock, F., Burrows, J. P., Vrekoussis, M., and Henze, D. K., Global budgets of
422 atmospheric glyoxal and methylglyoxal, and implications for formation of secondary organic aerosols, *J.*
423 *Geophys. Res.*, 113, 1-17, 2008.

424 Fu, T-M., Jacob, D. J., and Heald, C. L., Aqueous-phase reactive uptake of dicarbonyls as a source of organic
425 aerosol over eastern North America, *Atmos. Environ.*, 43, 1814–1822, 2009.

426 Gligorovski, S., and Herrmann, H.: Kinetics of reactions of OH with organic carbonyl compounds in aqueous
427 solution, *Phys. Chem. Chem. Phys.*, 6, 4118-4126, 10.1039/b403070b, 2004.

428 Glowa, G., Driver, P., and Wren, J. C.: Irradiation of MEK - II: A detailed kinetic model for the degradation under
429 of 2-butanone in aerated aqueous solutions steady-state gamma-radiolysis conditions, *Radiat. Phys. Chem.*,
430 58, 49-68, 10.1016/s0969-806x(99)00360-6, 2000.

431 Goldan, P. D., Kuster, W. C., Fehsenfeld, F. C., and Montzka, S. A.: Hydrocarbon measurements in the
432 southeastern United States: The Rural Oxidants in the Southern Environment (ROSE) program 1990, *Journal*
433 *of Geophysical Research-Atmospheres*, 100, 25945-25963, 10.1029/95jd02607, 1995.

434 Goldstein, A. H., and Galbally, I. E.: Known and unexplored organic constituents in the earth's atmosphere,
435 *Environmental Science & Technology*, 41, 1514-1521, 10.1021/es072476p, 2007.

436 Grosjean, D.: Formaldehyde and other carbonyls in Los-Angeles ambient air, *Environmental Science &*
437 *Technology*, 16, 254-262, 10.1021/es00099a005, 1982.

438 Grosjean, D., Swanson, R. D., and Ellis, C.: Carbonyls in Los-Angeles air - contribution of direct emissions and
439 photochemistry, *Sci. Total Environ.*, 29, 65-85, 10.1016/0048-9697(83)90034-7, 1983.

440 Grosjean, D., and Wright, B.: Carbonyls in urban fog, ice fog, cloudwater and rainwater, *Atmospheric*
441 *Environment*, 17, 2093-2096, 10.1016/0004-6981(83)90368-2, 1983.

442 Grosjean, D., Grosjean, E., and Moreira, L. F. R.: Speciated ambient carbonyls in Rio de Janeiro, Brazil,
443 *Environmental Science & Technology*, 36, 1389-1395, 10.1021/es0111232, 2002.

444 Hallquist, M., Wenger, J. C., Baltensperger, U., Rudich, Y., Simpson, D., Claeys, M., Dommen, J., Donahue, N.
445 M., George, C., Goldstein, A. H., Hamilton, J. F., Herrmann, H., Hoffmann, T., Iinuma, Y., Jang, M., Jenkin,
446 M. E., Jimenez, J. L., Kiendler-Scharr, A., Maenhaut, W., McFiggans, G., Mentel, T. F., Monod, A., Prevot,
447 A. S. H., Seinfeld, J. H., Surratt, J. D., Szmigielski, R., and Wildt, J.: The formation, properties and impact of
448 secondary organic aerosol: current and emerging issues, *Atmos. Chem. Phys.*, 9, 5155-5236, 2009.

449 Herrmann, H., Ervens, B., Nowacki, P., Wolke, R., and Zellner, R.: A chemical aqueous phase radical mechanism
450 for tropospheric chemistry, *Chemosphere*, 38, 1223-1232, 10.1016/s0045-6535(98)00520-7, 1999.

451 Herrmann, H., Tilgner, A., Barzagli, P., Majdik, Z., Gligorovski, S., Poulain, L., and Monod, A.: Towards a more
452 detailed description of tropospheric aqueous phase organic chemistry: CAPRAM 3.0, *Atmospheric*
453 *Environment*, 39, 4351-4363, 10.1016/j.atmosenv.2005.02.016, 2005.

454 Herrmann, H., Schaefer, T., Tilgner, A., Styler, S. A., Weller, C., Teich, M., and Otto, T.: Tropospheric
455 Aqueous-Phase Chemistry: Kinetics, Mechanisms, and Its Coupling to a Changing Gas Phase, *Chem. Rev.*,
456 115, 4259-4334, 10.1021/cr500447k, 2015.

457 Isidorov, V. A., Zenkevich, I. G., and Ioffe, B. V.: Volatile organic-compounds in the atmosphere of forests,
458 *Atmospheric Environment*, 19, 1-8, 10.1016/0004-6981(85)90131-3, 1985.

459 Kanakidou, M., Seinfeld, J. H., Pandis, S. N., Barnes, I., Dentener, F. J., Facchini, M. C., Van Dingenen, R.,
460 Ervens, B., Nenes, A., Nielsen, C. J., Swietlicki, E., Putaud, J. P., Balkanski, Y., Fuzzi, S., Horth, J., Moortgat,
461 G. K., Winterhalter, R., Myhre, C. E. L., Tsigaridis, K., Vignati, E., Stephanou, E. G., and Wilson, J.: Organic
462 aerosol and global climate modelling: a review, *Atmos. Chem. Phys.*, 5, 1053-1123, 2005.

463 Karl, T., Chahan, Y., Jordan, A., and Lindinger, W.: Dynamic measurements of partition coefficients using proton-
464 transfer-reaction mass spectrometry (PTR-MS), *International Journal of Mass Spectrometry*, 12269, 1-13,
465 2002.

466 Khalil, M. A. K., and Rasmussen, R. A.: Forest hydrocarbon emissions - relationships between fluxes and ambient
467 concentrations, *J. Air Waste Manage. Assoc.*, 42, 810-813, 1992.

468 Kirstine, W., Galbally, I., Ye, Y. R., and Hooper, M.: Emissions of volatile organic compounds (primarily
469 oxygenated species) from pasture, *Journal of Geophysical Research-Atmospheres*, 103, 10605-10619,
470 10.1029/97jd03753, 1998.

471 Kroll, J. H., Ng, N. L., Murphy, S. M., Varutbangkul, V., Flagan, R. C., and Seinfeld, J. H., Chamber studies of
472 secondary organic aerosol growth by reactive uptake of simple carbonyl compounds, *J. Geophys. Res.*, 110, 1-
473 10, 2005.

474 Lilie, J., Beck, G., and Henglein, A.: Pulse radiolysis of acetoin radicals and diacetyl anions in aqueous solution,
475 *Berichte Der Bunsen-Gesellschaft Fur Physikalische Chemie*, 72, 529-&, 1968.

476 Lin, G., Sillman, S., Penner, J. E., and Ito, A., Global modeling of SOA: the use of different mechanisms for
477 aqueous-phase formation, *Atmos. Chem. Phys.*, 14, 5451–5475, 2014.

478 Lipari, F., Dasch, J. M., and Scruggs, W. F.: Aldehyde emissions from wood-burning fireplaces, *Environmental*
479 *Science & Technology*, 18, 326-330, 10.1021/es00123a007, 1984.

480 Matthews, T. G., and Howell, T. C.: Visual colorimetric formaldehyde screening analysis for indoor air, *Journal*
481 *of the Air Pollution Control Association*, 31, 1181-1184, 1981.

482 Monod, A., Poulain, L., Grubert, S., Voisin, D., and Wortham, H.: Kinetics of OH-initiated oxidation of
483 oxygenated organic compounds in the aqueous phase: new rate constants, structure-activity relationships and
484 atmospheric implications, *Atmospheric Environment*, 39, 7667-7688, 10.1016/j.atmosenv.2005.03.019, 2005.

485 Monod, A., Chevallier, E., Jolibois, R. D., Doussin, J. F., Picquet-Varrault, B., and Carlier, P.: Photooxidation of
486 methylhydroperoxide and ethylhydroperoxide in the aqueous phase under simulated cloud droplet conditions,
487 *Atmospheric Environment*, 41, 2412-2426, 10.1016/j.atmosenv.2006.10.006, 2007.

488 Mopper, K., and Stahovec, W. L.: Sources and sinks of low-molecular-weight organic carbonyl-compounds in
489 seawater, *Mar. Chem.*, 19, 305-321, 10.1016/0304-4203(86)90052-6, 1986.

490 Morillon, V., Debeaufort, F., Jose, J., Tharrault, J. F., Capelle, M., Blond, G., and Voilley, A.: Water vapour
491 pressure above saturated salt solutions at low temperatures, *Fluid Phase Equilib.*, 155, 297-309,
492 10.1016/s0378-3812(99)00009-6, 1999.

493 Müller, K., van Pinxteren, D., Plewka, A., Svrčina, B., Kramberger, H., Hofmann, D., Bachmann, K., and
494 Herrmann, H.: Aerosol characterisation at the FEBUKO upwind station Goldlauter (II): Detailed organic
495 chemical characterisation, *Atmospheric Environment*, 39, 4219-4231, 10.1016/j.atmosenv.2005.02.008, 2005.

496 Pastina, B., and LaVerne, J. A.: Effect of molecular hydrogen on hydrogen peroxide in water radiolysis, *J. Phys.*
497 *Chem. A*, 105, 9316-9322, 10.1021/jp012245j, 2001.

498 Riemer, D., Pos, W., Milne, P., Farmer, C., Zika, R., Apel, E., Olszyna, K., Kliendienst, T., Lonneman, W.,
499 Bertman, S., Shepson, P., and Starn, T.: Observations of nonmethane hydrocarbons and oxygenated volatile
500 organic compounds at a rural site in the southeastern United States, *Journal of Geophysical Research-*
501 *Atmospheres*, 103, 28111-28128, 10.1029/98jd02677, 1998.

502 Rodigast, M., Mutzel, A., Iinuma, Y., Haferkorn, S., and Herrmann, H.: Characterisation and optimisation of a
503 sample preparation method for the detection and quantification of atmospherically relevant carbonyl
504 compounds in aqueous medium, *Atmos. Meas. Tech.*, 8, 2409-2416, 10.5194/amt-8-2409-2015, 2015.

505 Schaefer, T., Schindelka, J., Hoffmann, D., and Herrmann, H.: Laboratory Kinetic and Mechanistic Studies on
506 the OH-Initiated Oxidation of Acetone in Aqueous Solution, *J. Phys. Chem. A*, 116, 6317-6326,
507 10.1021/jp2120753, 2012.

508 Schütze, M., and Herrmann, H.: Uptake of acetone, 2-butanone, 2,3-butanedione and 2-oxopropanal on a water
509 surface, *Phys. Chem. Chem. Phys.*, 6, 965-971, 10.1039/b313474a, 2004.

510 Sebban, N., Bozzelli, J. W., and Bockhorn, H.: Thermochemistry and Kinetics for 2-Butanone-1-yl Radical (CH_2
511 center dot $\text{C}(=\text{O})\text{CH}_2\text{CH}_3$) Reactions with O_2 , *J. Phys. Chem. A*, 118, 21-37, 10.1021/jp408708u, 2014.

512 Sebban, N., Bozzelli, J. W., and Bockhorn, H.: Reactivity, thermochemistry and kinetics of 2-butanone radicals:
513 $\text{CH}_2\text{C}(=\text{O})\text{CHCH}_3$, $\text{CH}_3\text{C}(=\text{O})\text{CHCH}_3$ and $\text{CH}_3\text{C}(=\text{O})\text{CH}_2\text{CH}_2$, 2011.

514 Sempere, R., and Kawamura K.: Comparative distribution of dicarboxylic acids and related polar compounds in
515 snow, rain and aerosols from urban, *Atmos. Environ.*, 28, 449-459, 1994.

516 Singh, H. B., Salas, L. J., Chatfield, R. B., Czech, E., Fried, A., Walega, J., Evans, M. J., Field, B. D., Jacob, D.
517 J., Blake, D., Heikes, B., Talbot, R., Sachse, G., Crawford, J. H., Avery, M. A., Sandholm, S., and Fuelberg,
518 H.: Analysis of the atmospheric distribution, sources, and sinks of oxygenated volatile organic chemicals based
519 on measurements over the Pacific during TRACE-P, *Journal of Geophysical Research-Atmospheres*, 109, 20,
520 10.1029/2003jd003883, 2004.

521 Snider, J. R., and Dawson, G. A.: Tropospheric light alcohols, carbonyls and acetonitrile - concentrations in
522 southwestern united-states and henry law data, *Journal of Geophysical Research-Atmospheres*, 90, 3797-3805,
523 10.1029/JD090iD02p03797, 1985.

524 Stefan, M. I., and Bolton, J. R.: Reinvestigation of the acetone degradation mechanism in dilute aqueous solution
525 by the UV/H₂O₂ process, *Environmental Science & Technology*, 33, 870-873, 10.1021/es9808548, 1999.

526 Tan, Y., Carlton, A. G., Seitzinger, S. P., and Turpin, B. J.: SOA from methylglyoxal in clouds and wet aerosols:
527 Measurement and prediction of key products, *Atmospheric Environment*, 44, 5218-5226,
528 10.1016/j.atmosenv.2010.08.045, 2010.

529 van Pinxteren, D., Plewka, A., Hofmann, D., Müller, K., Kramberger, H., Svrčina, B., Bachmann, K., Jaeschke,
530 W., Mertes, S., Collett, J. L., and Herrmann, H.: Schmucke hill cap cloud and valley stations aerosol
531 characterisation during FEBUKO (II): Organic compounds, *Atmospheric Environment*, 39, 4305-4320,
532 10.1016/j.atmosenv.2005.02.014, 2005.

533 von Sonntag, C., and Schuchmann, H. P.: Aufklärung von Peroxyl-Radikalreaktionen in wäßriger Lösung mit
534 strahlenchemischen Techniken, *Angew. Chem.*, 130, 1255-1279, 1991.

535 von Sonntag, C., and Schuchmann, H. P.: Bimolecular Decay of peroxy radicals, in: *Peroxy radicals*, edited by:
536 Alfassi, Z. B., John Wiley & sons, 199-207, 1997.

537 Ware, G. W.: Methyl ethyl ketone, *Reviews of Environmental Contamination and Toxicology*, 106, 165-174,
538 1988.

539 Warneke, C., Karl, T., Judmaier, H., Hansel, A., Jordan, A., Lindinger, W., and Crutzen, P. J.: Acetone, methanol,
540 and other partially oxidized volatile organic emissions from dead plant matter by abiological processes:
541 Significance for atmospheric HO_x chemistry, *Glob. Biogeochem. Cycle*, 13, 9-17, 10.1029/98gb02428, 1999.
542 Yokelson, R. J., Burling, I. R., Gilman, J. B., Warneke, C., Stockwell, C. E., de Gouw, J., Akagi, S. K., Urbanski,
543 S. P., Veres, P., Roberts, J. M., Kuster, W. C., Reardon, J., Griffith, D. W. T., Johnson, T. J., Hosseini, S.,
544 Miller, J. W., Cocker, D. R., Jung, H., and Weise, D. R.: Coupling field and laboratory measurements to
545 estimate the emission factors of identified and unidentified trace gases for prescribed fires, *Atmos. Chem.*
546 *Phys.*, 13, 89-116, 10.5194/acp-13-89-2013, 2013.
547 Zegota, H., Schuchmann, M. N., Schulz, D., and Vonsonntag, C.: Acetylperoxy radicals, CH₃COCH₂O₂ - a
548 study on the gamma-radiolysis and pulse-radiolysis of acetone in oxygenated aqueous-solutions,
549 *Z.Naturforsch.(B)*, 41, 1015-1022, 1986.
550 Zhao, J., Levitt, N. P., Zhang, R., and Chen, J., Heterogeneous Reactions of Methylglyoxal in Acidic Media:
551 Implications for Secondary Organic Aerosol Formation, *Environ. Sci. Technol.*, 40, 7682-7687, 2006.
552 Zhou, X. L., and Mopper, K.: Apparent partition-coefficients of 15 carbonyl-compounds between air and seawater
553 and between air and fresh-water - implications for air sea exchange, *Environmental Science & Technology*,
554 24, 1864-1869, 10.1021/es00082a013, 1990.
555 Zhou, X. L., and Mopper, K.: Photochemical production of low-molecular-weight carbonyl compounds in
556 seawater and surface microlayer and their air-sea exchange, *Mar. Chem.*, 56, 201-213, 10.1016/s0304-
557 4203(96)00076-x, 1997.

558

Table 1: Conducted experiments in the bulk reactor.

Number of experiment	Type of experiment	Concentration precursor compound [mmol L ⁻¹]	Concentration H ₂ O ₂ [mmol L ⁻¹]	UV light ($\lambda = 254$ nm)	Reaction time [hours]	Number of repetition
1	Oxidation of MEK	0.1	2	✓	4	3
2	Reaction of H ₂ O ₂ with MEK	0.1	2	-	4	1
3	Photolysis of MEK	0.1	-	✓	4	1
4	Photolysis of H ₂ O ₂	-	2	✓	4	1
5	Oxidation of 2,3-butanedione	0.1	2	✓	4	1
6	Oxidation of hydroxyacetone	0.1	2	✓	4	1
7	Photolysis of 2,3-butanedione, hydroxyacetone, methylglyoxal	0.1	-	✓	4	1

MEK: Methyl ethyl ketone

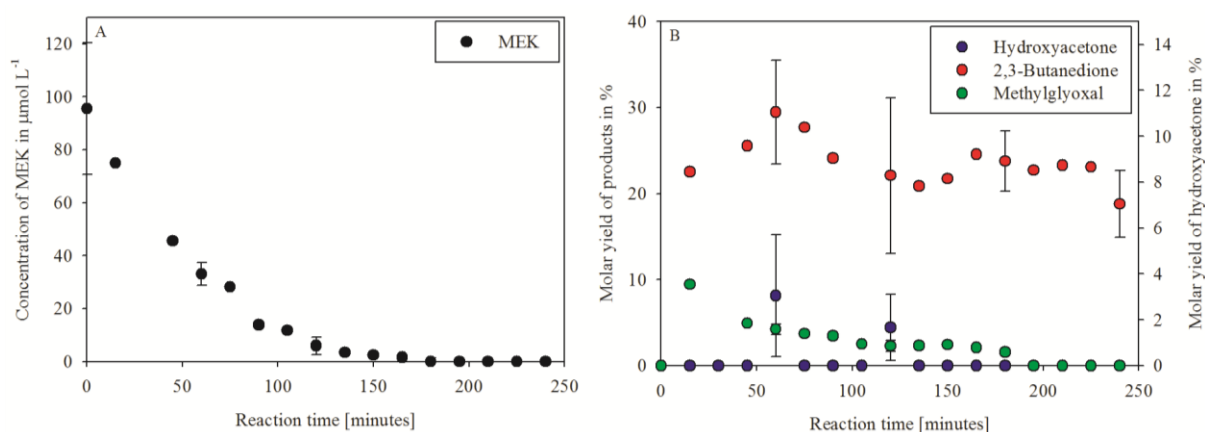


Figure 1: Consumption of MEK (A) during the oxidation with OH radicals and time-resolved formation of the products methylglyoxal (B), 2,3-butanedione (B), and hydroxyacetone (B).

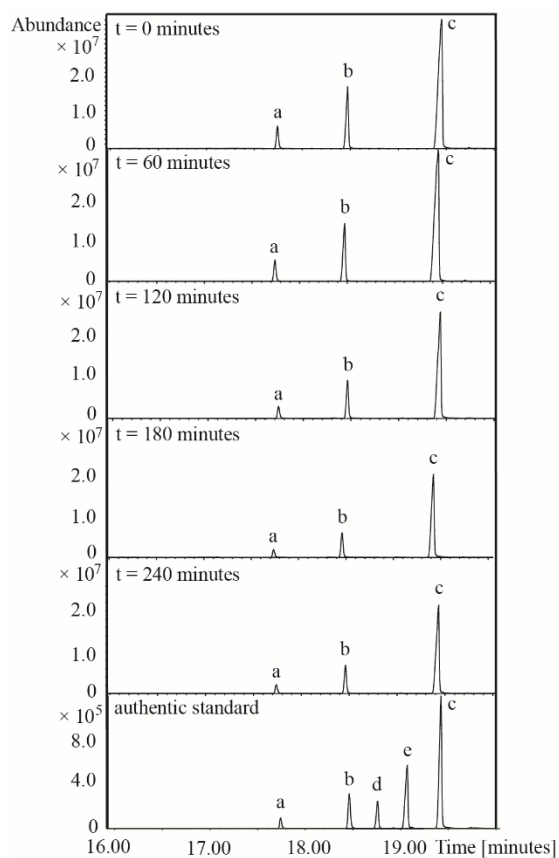


Figure 2: GC/MS chromatogram of oxidation of 2,3-butanedione (a,b,c) and the authentic standard compounds 2,3-butanedione (a,b,c) and methylglyoxal (d,e).

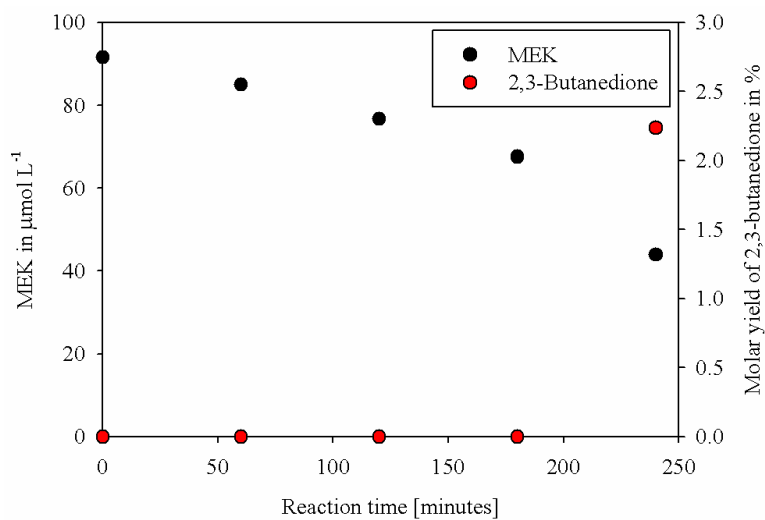


Figure 3: Photolysis of MEK and time-resolved formation of 2,3-butanedione.

Table 2: Maximal molar yields of the oxidation products.

Oxidation product	Maximal molar yield (± standard deviation) in %	Reaction time in minutes
2,3-Butanedione	29.5 ± 6.0	60
Methylglyoxal	9.5	15
Hydroxyacetone	3.0 ± 2.6	60

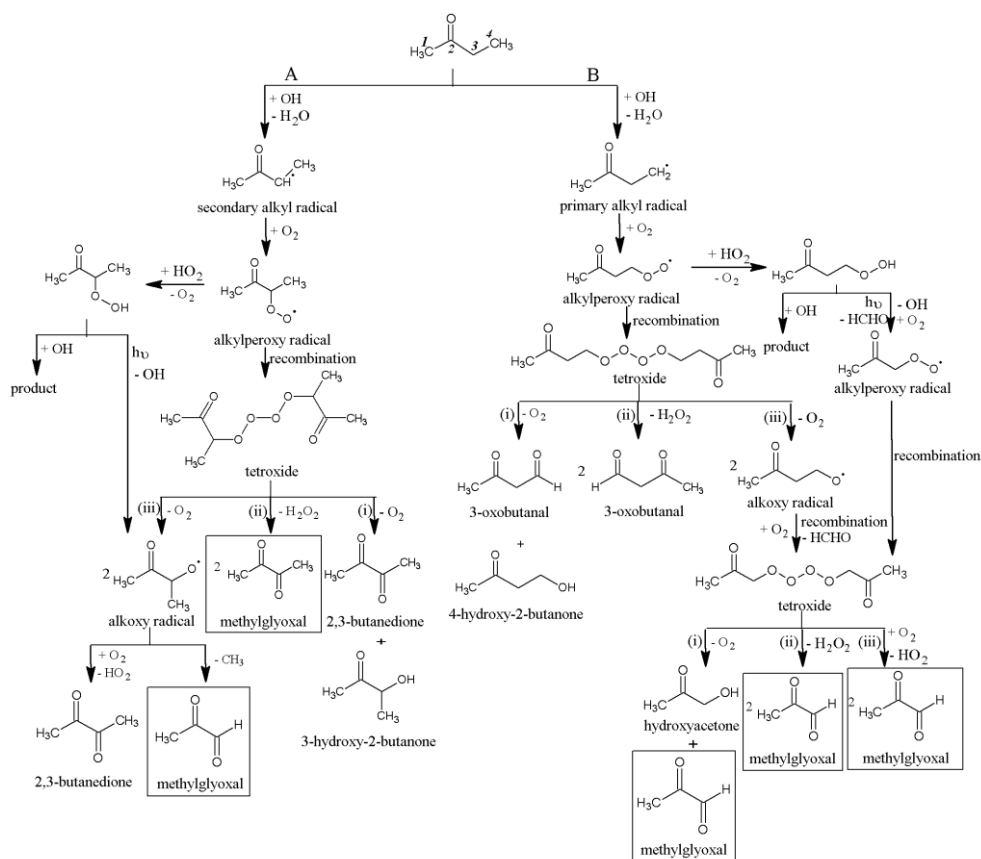


Figure 4: Recommendation of an oxidation mechanism of MEK for the formation of 2,3-butanedione, hydroxyacetone and methylglyoxal.

Table 3: Reaction mechanism and rate constants for the modelling of the experiment with COPASI.

	Reaction	Rate constant k	Comment
R1	$\text{H}_2\text{O}_2 + h\nu \rightarrow 2 \text{OH}$	$7.6 \times 10^{-6} \text{ s}^{-1}$	measured
R2	$2 \text{OH} \rightarrow \text{H}_2\text{O}_2$	$3.6 \times 10^9 \text{ M}^{-1} \text{ s}^{-1}$	Elliot and Buxton, 1992
R3	$\text{OH} + \text{H}_2\text{O}_2 \rightarrow \text{HO}_2 + \text{H}_2\text{O}$	$2.7 \times 10^7 \text{ M}^{-1} \text{ s}^{-1}$	Christensen et al., 1982
R4	$\text{OH} + \text{HO}_2 \rightarrow \text{H}_2\text{O} + \text{O}_2$	$6 \times 10^9 \text{ M}^{-1} \text{ s}^{-1}$	Elliot and Buxton, 1992
R5	$2 \text{HO}_2 \rightarrow \text{H}_2\text{O}_2 + \text{O}_2$	$9.8 \times 10^5 \text{ M}^{-1} \text{ s}^{-1}$	Christensen and Sehested, 1988
R6	$\text{HO}_2 + \text{H}_2\text{O}_2 \rightarrow \text{OH} + \text{O}_2 + \text{H}_2\text{O}$	$0.5 \text{ M}^{-1} \text{ s}^{-1}$	Pastina and LaVerne, 2001
R7	$\text{CH}_3\text{C}(\text{O})\text{CH}_2\text{CH}_3 + \text{OH} \rightarrow \text{CH}_3\text{C}(\text{O})\text{CH}_2\text{CH}_2 + \text{H}_2\text{O}$	$9 \times 10^8 \text{ M}^{-1} \text{ s}^{-1}$	changed after Gligorovski and Herrmann, 2004
R8	$\text{CH}_3\text{C}(\text{O})\text{CH}_2\text{CH}_3 + \text{OH} \rightarrow \text{CH}_3\text{C}(\text{O})\text{CHCH}_3 + \text{H}_2\text{O}$	$6 \times 10^8 \text{ M}^{-1} \text{ s}^{-1}$	changed after Gligorovski and Herrmann, 2004
R9	$\text{CH}_3\text{C}(\text{O})\text{CH}_2\text{CH}_2 + \text{O}_2 \rightarrow \text{CH}_3\text{C}(\text{O})\text{CH}_2\text{CH}_2\text{O}_2$	$3.1 \times 10^9 \text{ M}^{-1} \text{ s}^{-1}$	Zegota et al., 1986
R10	$2 \text{CH}_3\text{C}(\text{O})\text{CH}_2\text{CH}_2\text{O}_2 + \text{O}_2 \rightarrow \text{CH}_3\text{C}(\text{O})\text{CH}_2\text{O}_2 + 2 \text{HCHO}$	$4 \times 10^7 \text{ M}^{-1} \text{ s}^{-1}$	Zegota et al., 1986
R11	$2 \text{CH}_3\text{C}(\text{O})\text{CH}_2\text{O}_2 \rightarrow \text{CH}_3\text{C}(\text{O})\text{CH}_2\text{OH} + \text{CH}_3\text{C}(\text{O})\text{C}(\text{O})\text{H} + \text{O}_2$	$2 \times 10^8 \text{ M}^{-1} \text{ s}^{-1}$	Zegota et al., 1986
R12	$2 \text{CH}_3\text{C}(\text{O})\text{CH}_2\text{O}_2 \rightarrow 2 \text{HO}_2 + 2 \text{CH}_3\text{C}(\text{O})\text{C}(\text{O})\text{H}$	$4 \times 10^7 \text{ M}^{-1} \text{ s}^{-1}$	Zegota et al., 1986
R13	$2 \text{CH}_3\text{C}(\text{O})\text{CH}_2\text{O}_2 \rightarrow 2 \text{CH}_3\text{C}(\text{O})\text{C}(\text{O})\text{H} + \text{H}_2\text{O}_2$	$4 \times 10^8 \text{ M}^{-1} \text{ s}^{-1}$	Zegota et al., 1986
R14	$\text{CH}_3\text{C}(\text{O})\text{CH}_2\text{CH}_2\text{O}_2 + \text{HO}_2 \rightarrow \text{CH}_3\text{C}(\text{O})\text{CH}_2\text{CH}_2\text{OOH} + \text{O}_2$	$1 \times 10^7 \text{ M}^{-1} \text{ s}^{-1}$	Von Sonntag and Schuchmann, 1991
R15	$\text{CH}_3\text{C}(\text{O})\text{CH}_2\text{CH}_2\text{OOH} + \text{OH} \rightarrow \text{Product}$	$2.7 \times 10^7 \text{ M}^{-1} \text{ s}^{-1}$	Christensen et al., 1982
R16	$\text{CH}_3\text{C}(\text{O})\text{CH}_2\text{CH}_2\text{OOH} \rightarrow \text{OH} + \text{HCHO} + \text{CH}_3\text{C}(\text{O})\text{CH}_2$	$7.6 \times 10^{-7} \text{ s}^{-1}$	after Monod et al., 2007
R17	$\text{CH}_3\text{C}(\text{O})\text{CH}_2 + \text{O}_2 \rightarrow \text{CH}_3\text{C}(\text{O})\text{CH}_2\text{O}_2$	$3.1 \times 10^9 \text{ M}^{-1} \text{ s}^{-1}$	Zegota et al., 1986
R18	$2 \text{CH}_3\text{C}(\text{O})\text{CH}_2\text{O}_2 \rightarrow \text{CH}_3\text{C}(\text{O})\text{CH}_2\text{OH} + \text{CH}_3\text{C}(\text{O})\text{C}(\text{O})\text{H} + \text{O}_2$	$2 \times 10^8 \text{ M}^{-1} \text{ s}^{-1}$	Zegota et al., 1986
R19	$2 \text{CH}_3\text{C}(\text{O})\text{CH}_2\text{O}_2 \rightarrow \text{H}_2\text{O}_2 + 2 \text{CH}_3\text{C}(\text{O})\text{C}(\text{O})\text{H}$	$4 \times 10^8 \text{ M}^{-1} \text{ s}^{-1}$	Zegota et al., 1986
R20	$2 \text{CH}_3\text{C}(\text{O})\text{CH}_2\text{O}_2 \rightarrow 2 \text{CH}_3\text{C}(\text{O})\text{C}(\text{O})\text{H} + \text{HO}_2$	$4 \times 10^7 \text{ M}^{-1} \text{ s}^{-1}$	Zegota et al., 1986
R21	$\text{CH}_3\text{C}(\text{O})\text{CHCH}_3 + \text{O}_2 \rightarrow \text{CH}_3\text{C}(\text{O})\text{CHO}_2\text{CH}_3$	$3.1 \times 10^9 \text{ M}^{-1} \text{ s}^{-1}$	Glowa et al., 2000
R22	$2 \text{CH}_3\text{C}(\text{O})\text{CHO}_2\text{CH}_3 \rightarrow \text{O}_2 + \text{CH}_3\text{C}(\text{O})\text{C}(\text{O})\text{CH}_3 + \text{CH}_3\text{C}(\text{O})\text{CHCH}_3\text{OH}$	$2.5 \times 10^8 \text{ M}^{-1} \text{ s}^{-1}$	Glowa et al., 2000
R23	$2 \text{CH}_3\text{C}(\text{O})\text{CHO}_2\text{CH}_3 \rightarrow \text{H}_2\text{O}_2 + 2 \text{CH}_3\text{C}(\text{O})\text{C}(\text{O})\text{CH}_3$	$4.5 \times 10^8 \text{ M}^{-1} \text{ s}^{-1}$	Glowa et al., 2000
R24	$2 \text{CH}_3\text{C}(\text{O})\text{CHO}_2\text{CH}_3 \rightarrow \text{CH}_3\text{C}(\text{O})\text{C}(\text{O})\text{CH}_3 + \text{CH}_3\text{C}(\text{O})\text{C}(\text{O})\text{H} + \text{CH}_3 + \text{HO}_2$	$5 \times 10^7 \text{ M}^{-1} \text{ s}^{-1}$	Glowa et al., 2000
R25	$\text{CH}_3\text{C}(\text{O})\text{CHO}_2\text{CH}_3 + \text{HO}_2 \rightarrow \text{CH}_3\text{C}(\text{O})\text{CHOOHCH}_3 + \text{O}_2$	$1 \times 10^7 \text{ M}^{-1} \text{ s}^{-1}$	Von Sonntag and Schuchmann, 1991
R26	$\text{CH}_3\text{C}(\text{O})\text{CHOOHCH}_3 \rightarrow \text{CH}_3\text{C}(\text{O})\text{CHOCH}_3 + \text{OH}$	$7.6 \times 10^{-7} \text{ s}^{-1}$	after Monod et al., 2007
R27	$2 \text{CH}_3\text{C}(\text{O})\text{CHOCH}_3 \rightarrow \text{CH}_3\text{C}(\text{O})\text{C}(\text{O})\text{H} + \text{CH}_3\text{C}(\text{O})\text{C}(\text{O})\text{CH}_3 + \text{CH}_3 + \text{HO}_2$	$4 \times 10^7 \text{ M}^{-1} \text{ s}^{-1}$	Zegota et al., 1986
R28	$\text{CH}_3\text{C}(\text{O})\text{CHOOHCH}_3 + \text{OH} \rightarrow \text{Product}$	$2.7 \times 10^7 \text{ M}^{-1} \text{ s}^{-1}$	Christensen et al., 1982
R29	$\text{CH}_3\text{C}(\text{O})\text{C}(\text{O})\text{H} + \text{OH} \rightarrow \text{Product}$	$5.3 \times 10^8 \text{ M}^{-1} \text{ s}^{-1}$	Monod et al., 2005
R30	$\text{CH}_3\text{C}(\text{O})\text{C}(\text{O})\text{H} \rightarrow \text{Product}$	$3 \times 10^{-5} \text{ s}^{-1}$	measured
R31	$\text{CH}_3\text{C}(\text{O})\text{C}(\text{O})\text{CH}_3 + \text{OH} \rightarrow \text{Product}$	$1.4 \times 10^8 \text{ M}^{-1} \text{ s}^{-1}$	Gligorovski and Herrmann, 2004
R32	$\text{CH}_3\text{C}(\text{O})\text{C}(\text{O})\text{CH}_3 \rightarrow \text{Product} + 0.17 \text{CH}_3\text{C}(\text{O})\text{C}(\text{O})\text{H}$	$9 \times 10^{-6} \text{ s}^{-1}$	measured
R33	$\text{CH}_3\text{C}(\text{O})\text{CH}_2\text{OH} + \text{OH} \rightarrow \text{CH}_3\text{C}(\text{O})\text{C}(\text{O})\text{H}$	$8 \times 10^8 \text{ M}^{-1} \text{ s}^{-1}$	Stefan and Bolton, 1999
R34	$\text{CH}_3\text{C}(\text{O})\text{CH}_2\text{OH} \rightarrow \text{Product} + 0.19 \text{CH}_3\text{C}(\text{O})\text{C}(\text{O})\text{H}$	$2 \times 10^{-5} \text{ s}^{-1}$	measured
R35	$\text{CH}_3\text{C}(\text{O})\text{CH}_2\text{CH}_3 \rightarrow \text{Product} + 0.02 \text{CH}_3\text{C}(\text{O})\text{C}(\text{O})\text{CH}_3$	$5 \times 10^{-5} \text{ s}^{-1}$	measured

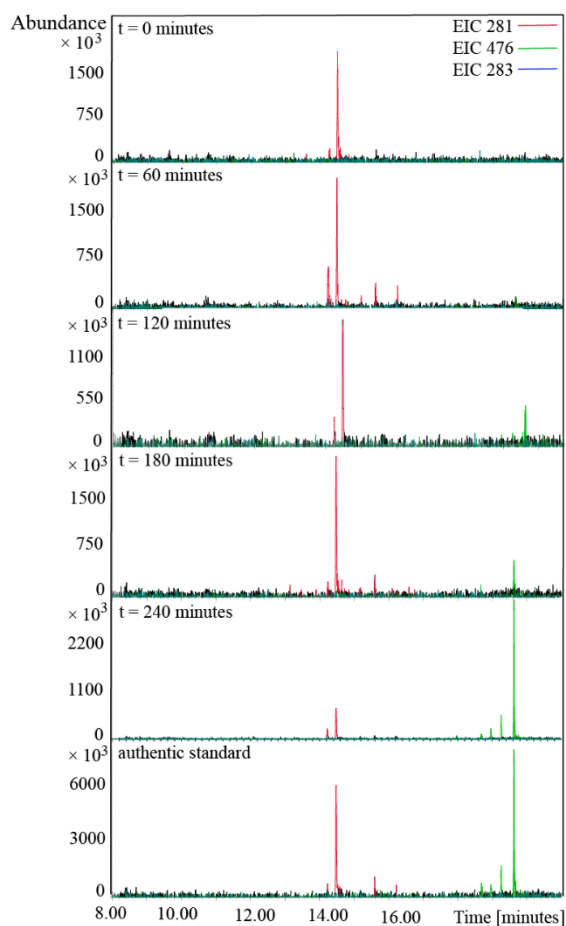


Figure 5: Extracted ion chromatogram (EIC) of m/z 281 M^{+} , m/z 476 M^{+} and m/z 283 M^{+} during the oxidation of MEK and EIC of the authentic standard compounds.

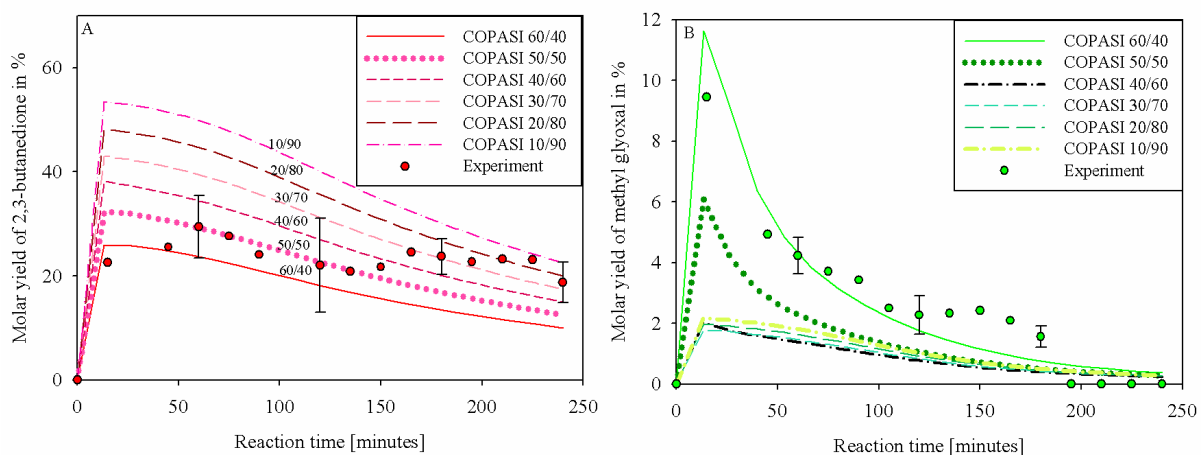


Figure 6: Comparison of the molar yields of 2,3-butanedione (A) and methylglyoxal (B) for the model and experimental results using different branching ratios of the primary/secondary H-atom abstraction varied between 60/40 up to 10/90.

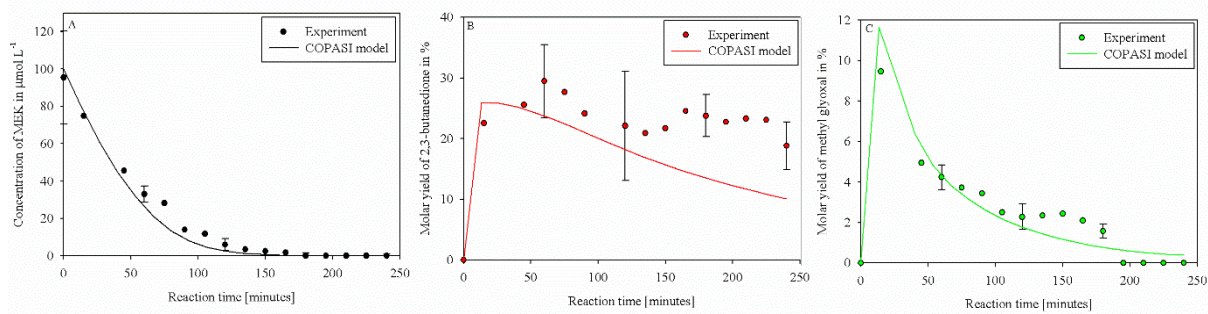


Figure 7: Comparison of the model and experimental results for MEK (A), 2,3-butanedione (B), and methylglyoxal (C).